




## Article

# New Records of *Tetraselmis* sp. Strains with Biotechnological Potential Isolated from Greek Coastal Lagoons

Alexandros Ntzouvaras <sup>1,2</sup>, Xanthi Chantzistroutsiou <sup>1,\*</sup>, Niki Papageorgiou <sup>2</sup>, Aikaterini Koletti <sup>2</sup> , Ioannis-Dimosthenis Adamakis <sup>3</sup> , Maria-Eleftheria Zografaki <sup>2</sup>, Sofia Marka <sup>2</sup>, Gabriel Vasilakis <sup>2</sup> , Amerssa Tsirigoti <sup>1</sup>, Ioannis Tzovenis <sup>1</sup>, Emmanouil Flemetakis <sup>2</sup> and Athena Economou-Amilli <sup>1</sup>

<sup>1</sup> Section of Ecology & Systematics, Department of Biology, School of Science, National and Kapodistrian University of Athens, Panepistimiopolis Zografou, 15784 Athens, Greece; alexntzouv@gmail.com (A.N.)

<sup>2</sup> Department of Biotechnology, School of Applied Biology and Biotechnology, Agricultural University of Athens, 11855 Athens, Greece

<sup>3</sup> Section of Botany, Department of Biology, School of Science, National and Kapodistrian University of Athens, 15784 Athens, Greece

\* Correspondence: xchantzi@biol.uoa.gr; Tel.: +30-6949177297

**Abstract:** In the pursuit of sustainable sources for food, energy, and health products, microalgae have gained attention. In the present study, the lagoonal system of the Nestos River delta was selected as a sampling point in order to search for opportunistic and robust species. Two new strains of *Tetraselmis* are described with regards to their taxonomic features (as observed using light and transmission electron microscopy and molecular phylogenetics) and their biochemical properties (total lipid, total protein, and total carbohydrate content, photosynthetic pigments, and antioxidant capacity). The studied strains were identified as representatives of *Tetraselmis verrucosa* f. *rubens*. Furthermore, both strains exhibited an interesting biochemical profile coupled with high growth rates and promising antioxidant activity, without the use of enhancement and induction culture methods, warranting further investigation and showing potential for biotechnological use.

**Keywords:** microalgae; microalgal strains; *Tetraselmis*; *T. verrucosa* f. *rubens*; algal culture; taxonomy; antioxidant capacity



**Citation:** Ntzouvaras, A.; Chantzistroutsiou, X.; Papageorgiou, N.; Koletti, A.; Adamakis, I.-D.; Zografaki, M.-E.; Marka, S.; Vasilakis, G.; Tsirigoti, A.; Tzovenis, I.; et al. New Records of *Tetraselmis* sp. Strains with Biotechnological Potential Isolated from Greek Coastal Lagoons. *Water* **2023**, *15*, 1698. <https://doi.org/10.3390/w15091698>

Academic Editor: Guangyi Wang

Received: 22 March 2023

Revised: 19 April 2023

Accepted: 22 April 2023

Published: 27 April 2023



**Copyright:** © 2023 by the authors. Licensee MDPI, Basel, Switzerland. This article is an open access article distributed under the terms and conditions of the Creative Commons Attribution (CC BY) license (<https://creativecommons.org/licenses/by/4.0/>).

## 1. Introduction

The Earth's environments are facing a series of challenges, mainly derived from the uncontrollably increasing human population and climate crisis. Food, health, and fuel industries aim to develop new sustainable products in order to cover humanity's constantly rising needs. Blue biotechnology is an alternative approach emphasizing the importance of exploring insufficiently studied marine biodiversity and exploiting it through environmentally friendly technologies. Microalgae, with more than 300,000 different species, are known to serve as a renewable source for a plethora of valuable products, although they remain a mostly untapped and fragmentarily studied resource [1].

Transitional waters, such as lagoons and estuaries, are significant ecological systems that, due to high spatio-temporal variability and anthropogenic pressure, favor the development of opportunistic microalgal species [2]. The impact of the variability and fluctuation of abiotic factors on lagoonal phytoplankton is expressed through high productivity rates, tolerance to intense abiotic factor gradients (e.g., nutrients, salinity, temperature, and light intensity), and unique biochemical properties [3]. As a result, the systematic investigation of these environments could reveal new robust strains with interesting bioactive compounds.

The present study aims to introduce selected strains isolated from Greek lagoons that produce high-added value compounds (antioxidants, oils, bioactive polysaccharides, and pigments) with biotechnological applications. In this framework, a sampling excursion took

place in Vistonida Lake at the Nestos Delta lagoonal system in northern Greece, followed by the isolation and characterization of two *Tetraselmis* Stein (1878) strains. *Tetraselmis* as a genus is a typical representative of transitional ecosystems, while its biotechnological potential has been extensively reviewed (e.g., [4–7]). In the past few decades, the presence of the form *Tetraselmis verrucosa* f. *rubens* (Butcher) Hori, Norris, and Chihara (1983) has been verified in many Greek coastal lagoons and representatives of the taxon have been taxonomically and biochemically investigated [5]. In addition, *Tetraselmis* is of particular taxonomic interest as it is the only extant genus, along with the genus *Scherffelia* Pascher (1911), comprising the class Chlorodendrophyceae [8]. Here, the morphological, molecular, and biochemical features of two novel Greek *Tetraselmis* strains are presented, while their potential industrial interest is discussed.

## 2. Materials and Methods

### 2.1. Sampling

The studied strains were isolated from water samples from the lagoons of “Ksirolimni” (40°57′ N 25°09′ E) and “Porto Lagos” (40°58′ N 25°09′ E). The sampled lagoons are part of the estuarine system of Nestos River (Nestos Delta National Park) in northern Greece (Figure 1). The Nestos Delta is one of the most ecologically significant areas in Greece, covering an area of approximately 550 km<sup>2</sup> with a catchment basin of 5749 km<sup>2</sup>, 40% of which extends within Greek territory [9]. The area is protected by national and international legislation including the Bern Convention, EC directives, and the Natura 2000 Network and it was included in the Ramsar Convention in 1971 [10,11]. The coverage area of each lagoon and some physical and chemical measurements of each sampling site are shown in Table 1.

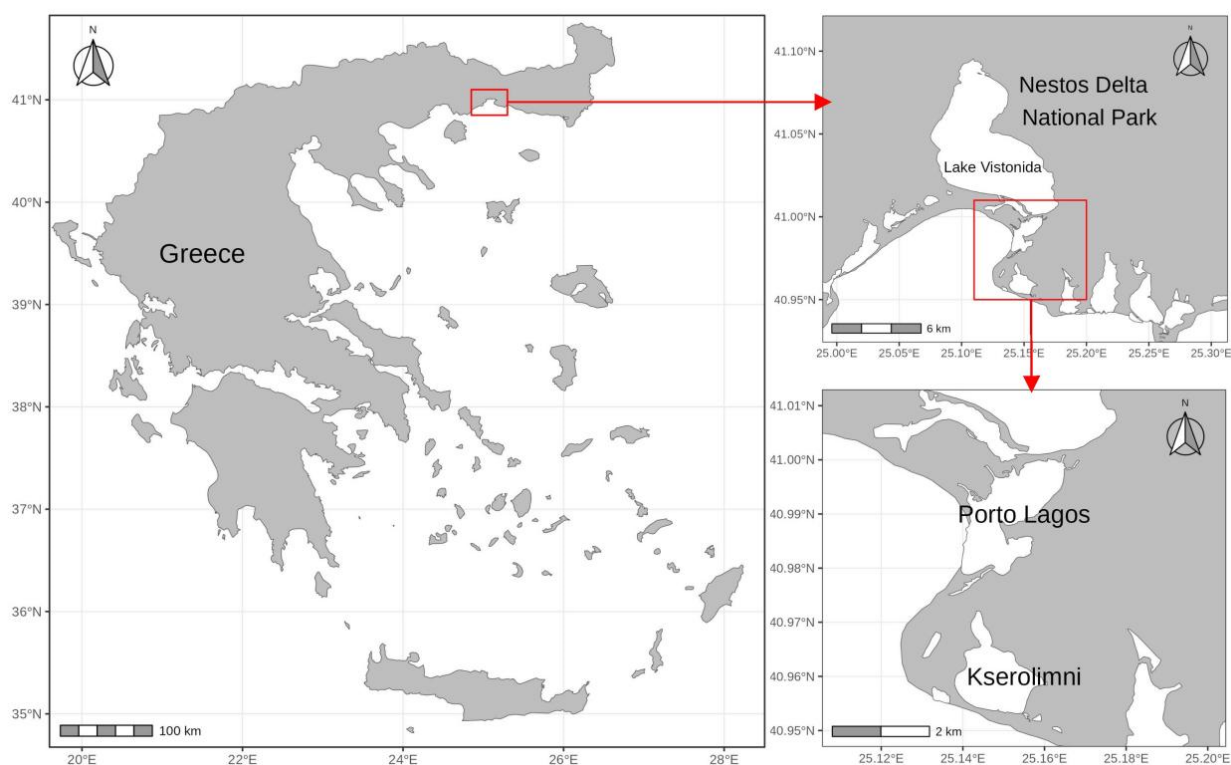


**Figure 1.** A map showing the location of the Nestos Delta National Park in northern Greece (Macedonia and Thrace) and the coastal lagoons “Porto Lagos” and “Ksirolimni” where the sampling took place.

**Table 1.** Physical and chemical parameters of the water sampled from the lagoons “Porto Lagos” and “Ksirolimni”. Temperature (T), pH, conductivity (CND), salinity (S), and dissolved oxygen (DO) were measured on site during sampling. Surface area (SA), perimeter (P), and maximum depth (MD) data sources: [12,13].

Lagoon	SA (km <sup>2</sup> )	P (km)	MD (m)	T(°C)	CND (mS)	S (‰)	DO (mg·L <sup>-1</sup> )
Porto Lagos (PLA)	13	-	-	23.7	8.04	64.8	49
Ksirolimni (KSI)	1.90	5.8	1.0	23.9	8.22	63.0	47

Samplings were carried out during October 2020 using a custom-made water sampler (as the two lagoons are rather shallow, with a maximum depth  $\leq 1$  m) and samples were taken from a depth of 0.5 m. The sampled water was filtered using a fine plankton net with a mesh of 25 microns in order to remove grazing zooplankton and large phytoplankton cells. The samples were then transferred to the lab in 1 L screwcap plastic bottles using isothermal containers. Certain physical and chemical parameters (temperature, pH, dissolved oxygen, conductivity, and salinity) of the sampling stations were measured on site (Table 1) using a Lovibond SensoDirect 150 system (Tintometer Ltd., Lovibond® Water Testing, Amesbury, UK) and an Atago S/Mill-E (Atago CO., Ltd., Tokyo, Japan) handheld salinity refractometer.

## 2.2. Strain Isolation and Cultivation

The live field water samples were enriched with L1-medium [14] (see Supplemental File S1) and were incubated in the lab under natural sunlight. The resulting natural algal blooms (NABs) contained several different algal taxonomic groups. Strain selection was carried out using a Zeiss KF2 light microscope (Carl Zeiss AG, Jena, Germany) at  $\times 200$ ,  $\times 400$ , and  $\times 1000$  magnification. Strain isolation was carried out with 3 different techniques: (a) multiple dilution, (b) agar plating, and (c) capillary single-cell isolation using a micropipette [15]. For the isolation stages, autoclaved artificial saltwater of adjusted salinity (Tropic Marin® PRO-REEF sea salt formula, Tropic Marin AG, Hünenberg, Switzerland) enriched with L1-medium was used. The single-strain, non-axenic cultures are preserved in the AthU-AI (Athens University Algae) strain bank of the NKUA (National and Kapodistrian University of Athens, <http://phycotheca.biol.uoa.gr>, accessed on 1 April 2023) in a closed culture chamber with steady conditions (temperature: 21–23 °C, light intensity: 100–150  $\mu\text{moles photons}\cdot\text{m}^{-2}\cdot\text{s}^{-1}$ , light period: 12 h day–12 h night, relative humidity: ~35%) and are re-cultivated on a monthly basis under sterile conditions in a Laminar Flow Cabinet (LFC). The two *Tetraselmis* sp. strains studied herein are preserved in sterile saltwater of adjusted salinity (40‰) enriched with Walne’s medium [14] (see Supplemental File S1).

## 2.3. Microscopic Observation and Morphology

Cells of all strains were observed under light microscopy (LM) and photographed using (a) a Zeiss Axiolab E re microscope equipped with an AmScope MU503 digital camera and the accompanying PC software (v4.11.04022022, AmScope, Irvine, CA, USA) and (b) a Zeiss Axioplan microscope equipped with an MRc 5 Axiocam digital camera (Zeiss, Jena, Germany), an epifluorescence system, and differential interference contrast system (Nomarski). Living cells were observed at  $\times 200$ ,  $\times 400$ , and  $\times 1000$  magnification and their morphological description and identification was based on the keys by Norris et al. [16] and Hori et al. [17]. Cell biometry was carried out by measuring the cell height (H) and width (W) of  $\times 1000$  magnified fixed cells, and cell biovolume was calculated according to Hillebrand et al. [18]. A minimum of 30 cells per strain were measured, while those cells considered as non-representative of the strain due to irregular shape, wrong positioning, or damage were not included.

For transmission electron microscopy (TEM), cultured *Tetraselmis* cells were centrifuged, collected, enclosed in low melting agarose pellets, and fixed in 2% (*v/v*) glutaraldehyde (Sigma, Darmstadt, Germany) in 50 mM sodium cacodylate buffer (pH 7) for 4 h at 4 °C. Afterwards, cells were post-fixed in 1% (*w/v*) osmium tetroxide for 12 h and dehydrated in a graded ethanol series (10, 20, 30, 50, 70, 90, 100%) before finally being embedded in Spurr's resin (PolySciences, Niles, IL, USA). Ultrathin sections (60–80 nm) were taken with either a Reichert-Jung ULTRACUT E (Reichert-Jung Optical Company, Vienna, Austria) or an ULTRATOME III TYPE 8801A ultramicrotome (LKB, Stockholm, Sweden) with a diamond knife. Prior to observation, sections were stained with 4% uranyl acetate (*w/v*) and 1% lead citrate (*w/v*). The sections were examined with a JEOL JEM 1011 TEM at 80 kV, and electron micrographs were acquired with a Gatan ES500W digital camera according to the manufacturer's instructions.

#### 2.4. Molecular Methods

Extraction of total DNA from single unialgal cultures of all strains was performed using the "Genomic DNA from Soil" kit (Macherey Nagel, Düren, Germany) according to the manufacturer's protocol. Polymerase Chain Reaction (PCR) for the *18S* rRNA, *ITS* (internal transcribed spacer), *rbcL* (large subunit of ribulose-1,5-bisphosphate carboxylase-oxygenase or RuBisCO), and *TufA* (elongation factor Tu) fragments were conducted with a reaction volume of 25 µL, using 0.5 µL of each primer (Table 2), 2 µL of the samples, and 12.5 µL of OneTaq 2X Master Mix with Standard Buffer (New England Biolabs, Ipswich, MA, USA) and adjusting the volume with double-distilled water (ddH<sub>2</sub>O). The amplification reactions were optimized for microalgal-derived gene fragments; more specifically, the PCR comprised an initial denaturation step at 95 °C for 3 min followed by 40 cycles consisting of 94 °C for 15 s, 48 °C for 1 min, and 72 °C for 1.5 min and a 10 min final extension step at 72 °C. PCR amplicons were quantified with a Spectrophotometer NanoDrop ND-1000 (Thermo Scientific, Waltham, MA, USA) and run in a 1.5% agarose gel stained with ethidium bromide. The "NucleoSpin Gel and PCR Clean-up" kit (Macherey Nagel) was used for the purification of each fragment according to the manufacturer's protocol. Automated sequencing of both strands of each PCR amplicon was performed in an automated sequencer (using Big-Dye terminator chemistry) with the same primers that were used for the PCR amplifications.

**Table 2.** Primer sequences used for molecular taxonomy analysis.

Gene	Primer	Sequence	Reference
<i>18S</i>	MA1	5'-CGGGATCCGTAGTCATATGCTTGTCTC-3'	Olmos-Soto et al., 2012 [19]
	MA2	5'-CGGAATTCCTTCTGCAGGTTACC-3'	
	DSs	5'-GCAGGAGAGCTAATAGGA-3'	
<i>rbcL</i>	<i>rbcL</i> 475–497	5'-CGTGACAACTAAACAAATATGG-3'	Nozaki et al., 1995 [20]
	<i>rbcL</i> 1181–1160	5'-AAGATTTCAACTAAAGCTGGCA-3'	Assunção et al., 2012 [21]
<i>ITS</i> region	ITS1	5'-TCCGTAGGTGAACCTGCGG-3'	Preetha et al., 2012 [22]
	ITS4	5'-TCCTCCGCTTAT-TGATATGC-3'	
<i>tufA</i>	TufA F	5'-TGAAACAGAAAWCGTCATTATGC-3'	Vieira et al., 2016 [23]
	TufA R	5'-CCTTCNCGAATMGCRAAWCGC-3'	

The generated sequences were edited in DNA Baser v5.08 (Heracle BioSoft SRL, Lilienthal, Germany) and evaluated for their homology to the respective gene sequences available in GenBank [24] through a BLAST search. A dataset compiled from the sequences generated in the present study sequences, as well as selected BLAST results (similarity >98%, query cover >80%), was used for the subsequent phylogenetic analysis. Sequences were aligned using Mega X v10.2.6 and the Clustal X algorithm. Phylogeny was performed within a Bayesian framework (BI) using Mega X v10.2.6 [25]. For the concatenated *tufA-rbcL* tree, the Maximum Likelihood method, General Time Reversible model [26], and a discrete

Gamma distribution were used to model evolutionary rate differences among sites. The rate variation model allowed for some sites to be evolutionarily invariable. For the *ITS* region, the Maximum Likelihood method, Kimura 2-parameter model [27], and a discrete Gamma distribution were used. For the *rbcL* and *TufA* genes, the Maximum Likelihood method and General Time Reversible model [27] were used. The rate variation model allowed for some sites to be evolutionarily invariable.

### 2.5. Culture Kinetics

Triplicate batch cultures of all strains were gradually scaled up from 50 mL to 2 L of rigorously aerated (0.5–1 vvm flow rate, air only), autoclaved artificial salt water (adjusted to 40‰ salinity) enriched with Walne's medium. Artificial illumination was provided by cool daylight fluorescent lamps at 150–200  $\mu\text{mol photons m}^{-2}\cdot\text{s}^{-1}$  (12:12 h L/D), while the temperature was kept constant at  $22 \pm 1$  °C. Culture cell density ( $N_t$ , cells·mL<sup>-1</sup>) was measured daily under a Zeiss KF2 light microscope using an improved Neubauer hemocytometer to obtain each strain's growth curve and determine maximum growth rates ( $\mu_{\text{max}} = [\ln(N_t/N_0)]/\Delta t$ ). To calculate volumetric biomass yield and productivity, cell dry weight (DW) was determined for each strain and multiplied by cell density. DW was determined by filtering a certain culture volume of known cell density on pre-weighed GF/C filters (Whatman, Maidstone, UK) under vacuum, rinsing it thoroughly with isotonic ammonium formate solution, and then drying it in a NÜVE FN 500 furnace (NÜVE, Ankara, Turkey) at 60 °C overnight. Subsequently, DW was determined by weighing the dried filters on a Sartorius 5-digit electronic scale (Sartorius AG, Göttingen, Germany).

### 2.6. Biochemical Analyses

#### 2.6.1. Total Protein Content (TP)

Total nitrogen was estimated through the Kjeldahl method [28]. The Kjeldahl method is based on three consecutive steps: digestion, distillation, and titration. Digestion was carried out on a Labtec DT 220 (FOSS A/S, Hillerød, Denmark) digester, while a Tecator Kjeltec 8200 (FOSS A/S, Hillerød, Denmark) unit was used for distillation. Crude protein was calculated by multiplying total nitrogen by the traditional protein conversion factor of 6.25 [29].

#### 2.6.2. Total Lipid Content (TL)

The Sulpho-Phospho-Vanillin reaction (SPV) colorimetric method [30] was used to determine the total fatty acid fraction. Initially, the phospho-vanillin solution was prepared, and the next step was to plot the standard curve for which known amounts of pure analytical grade cholesterol (0.05, 0.1, 0.25, 0.5, and 1 mg) were used. For analysis of the studied samples, 5–10 mg of dried biomass was weighed with a 5-digit precision scale (Pioneer, Ohaus GmbH, Parsipanny, NJ, USA) and transferred to glass test tubes. A volume of 2 mL of concentrated sulfuric acid (95–97%) was added to each sample and the samples were placed in a hot bath (100 °C) for 15 min. After 15 min, the samples were allowed to cool at room temperature for 5 min and 5 mL of phospho-vanillin was added. A gentle agitation step followed this procedure and the samples were then placed in a shaker at 200 rpm at 37 °C for 15 min. The samples were then diluted 1:5 with a 60% phosphoric acid solution. After dilution, an equal amount of each sample was transferred to a 96-well plate (3 replicates for each sample), which was measured at a wavelength of 530 nm using an Infinite 200 PRO plate reader (Tecan, Männedorf, Switzerland).

#### 2.6.3. Total Polysaccharide Content (PS)

For quantitative determination of the total polysaccharide fraction (intracellular and extracellular cell-bounded polysaccharides) of the dried biomass, the colorimetric method of phenol–sulfuric acid was used, as described by DuBois et al. [31]. The method involves the addition of 1 mL of phenol (5% *w/v*) and 5 mL of sulfuric acid (95–97%) to 1 mL of suitably diluted biomass suspension (4 g·L<sup>-1</sup>), diluted tenfold (sugar concentration limits

0.01–0.10 g·L<sup>-1</sup>) in a test tube, and the mixture was allowed to react at a temperature of 20–30 °C after stirring for a period of 10 to 20 min, with intermediate re-stirring between intervals. The orange complex formed was measured photometrically at a wavelength of 490 nm with a Hitachi U-2000 spectrophotometer (Hitachi Ltd., Tokyo, Japan), and the concentration of total sugars was determined (as glucose equivalents) through a standard reference curve of known glucose concentrations (0.01 g·L<sup>-1</sup>, 0.03 g·L<sup>-1</sup>, 0.05 g·L<sup>-1</sup>, 0.06 g·L<sup>-1</sup>, 0.08 g·L<sup>-1</sup>, and 0.1 g·L<sup>-1</sup>).

#### 2.6.4. Pigment Analysis

To estimate the production of total carotenoids (TC) and chlorophylls a (Chl *a*) and b (Chl *b*), the extraction of pigments was carried out in 80% acetone, followed by spectrophotometry using an ONDA 135 UV-21 photometer (Giorgio Bormac s.r.l., Carpi, Italy). A sample of 5 mL was taken from each culture and centrifuged for 10 min at 3000 rpm. After the centrifugation, the supernatant was discarded, and 5 mL of 80% acetone was added to the pellet followed by vortexing in order to facilitate pigment extraction. The extracted samples were stored in a freezer (4 °C) overnight. The optical density (OD) of the extracts was measured at 470 nm for carotenoids and at 645, 646, 662, and 663 nm for chlorophylls using 80% acetone as a blank. The equations of Borovkov [32] are given below.

$$\text{Chl } a = 12.21 \times \text{OD}_{663} - 2.81 \times \text{OD}_{646} \quad (1)$$

$$\text{Chl } b = 20.13 \times \text{OD}_{646} - 5.03 \times \text{OD}_{663} \quad (2)$$

$$\text{TC} = (1000 \times \text{OD}_{470} - 3.27 \times \text{Chl } a - 104 \times \text{Chl } b)/198 \quad (3)$$

Those of Wellburn [33] are as follows:

$$\text{Chl } a = 11.75 \times \text{OD}_{662} - 2.35 \times \text{OD}_{645} \quad (4)$$

$$\text{Chl } b = 18.61 \times \text{OD}_{645} - 3.96 \times \text{OD}_{662} \quad (5)$$

$$\text{TC} = (1000 \times \text{OD}_{470} - 2.27 \times \text{Chl } a - 81.4 \times \text{Chl } b)/227 \quad (6)$$

These equations were then used to estimate the concentration of chlorophylls and total carotenoids expressed in mg·L<sup>-1</sup>.

#### 2.7. Antioxidant Capacity

For estimation of the antioxidant capacity of the strains, total phenolic content (TPC) [34] and total flavonoid content (TFC) [35] were estimated, and two different assays were used: (a) FRAP (Ferric Reducing Antioxidant Power) [36] and (b) TEAC (Trolox Equivalent Antioxidant Capacity) [37].

The first step was the preparation of extracts from each strain, with 0.5 g of freeze-dried biomass dissolved in 500 mL of pure methanol (MeOH). Initially, the samples were mechanically stirred for 10 s at 7 rpm and then placed for 20 min in an ultrasonic bath (70% and 15 °C), followed by centrifugation for 10 min at 13,000 rpm and 4 °C. Subsequently, 300 µL of supernatant was transferred to autoclaved test tubes and the procedure was repeated for the remaining pellet, leading to a total of 600 µL of extract for each strain. Finally, 200 µL was filtered using a 0.22 µm filter and then placed on a rotator evaporator to evaporate the methanol. For each strain, five replicates were used and the samples were stored at -20 °C until use.

### 2.7.1. TPC

For estimation of the phenolic content (TPC) of the extracts, the Folin–Ciocalteu method was used [34]. Initially, Folin–Ciocalteu reagent (Sigma-Aldrich, St. Louis, MO, USA) was diluted at a ratio of 1:10 in deionized water and a sodium carbonate solution (0.5 M) was prepared. Next, 10  $\mu\text{L}$  of each sample ( $1\text{ mg}\cdot\text{mL}^{-1}$ ), 95  $\mu\text{L}$  of Folin–Ciocalteu reagent, and 95  $\mu\text{L}$  of sodium carbonate solution (0.5 M) was added in a 96-well plate. Finally, the samples were measured photometrically at 765 nm 5 times in total at 30 min intervals at room temperature using pure methanol as a blank. The total phenolic content was calculated in gallic acid equivalents per gram of dry matter, based on a gallic acid standard reference curve.

### 2.7.2. TFC

For the estimation of total flavonoids, two basic reagents were prepared: (a) pure methanol with 5% ethanoate acid *v/v* (acetic acid,  $\text{CH}_3\text{COOH}$ ) and (b) 2% aluminum trichloride ( $\text{AlCl}_3$ ) dissolved in methanol. Subsequently, 20  $\mu\text{L}$  of each sample and 160  $\mu\text{L}$  of reagent A was then added in a 96-well plate and measured photometrically at 420 nm. Afterwards, 20  $\mu\text{L}$  of reagent B was added and the samples were measured photometrically again at 420 nm. Methanol was used as a blank in both measurements. Finally, to estimate total flavonoids, the difference between the two measurements was calculated and the results were expressed as mg quercetin equivalents per gram of dry biomass based on a quercetin standard curve.

### 2.7.3. FRAP

FRAP reagent was prepared using the following solutions in a 10:1:1 ratio: (i) 0.3 M sodium acetate solution ( $\text{CH}_3\text{COONa}\cdot 3\text{H}_2\text{O}$ ) at pH 3.6, (ii) 10 mM solution of the reagent tripyridyltriazine (TPTZ), and (iii) 20 mM ferric chloride solution ( $\text{FeCl}_3\cdot 6\text{H}_2\text{O}$ ). Subsequently, 10  $\mu\text{L}$  of each strain extract was diluted in methanol at a ratio of 1:5, and after the addition of 190  $\mu\text{L}$  of FRAP reagent, the samples were placed in a 96-well plate and incubated at 37 °C for 30 min. Finally, the absorbance of each sample was measured at 593 nm, using a solution of FRAP reagent in the extraction solvent (i.e., methanol) as a blank, and the total antioxidant capacity of each sample was calculated as ascorbic acid equivalents (in  $\mu\text{M}$ ).

### 2.7.4. TEAC

For the TEAC assay, concentrated potassium persulfate (2.45 mM) was added to a 7 mM ABTS solution (Sigma-Aldrich, St. Louis, MO, USA). The final solution was incubated at room temperature for 12–16 h before use. The solution was then diluted in ethanol until an absorbance of  $0.7 \pm 0.02$  at 734 nm was obtained. Subsequently, 10  $\mu\text{L}$  of each extract mixed with 200  $\mu\text{L}$  of the final ABTS solution was placed in a 96-well plate and incubated for up to 20 min at 30 °C under constant shaking, and optical density was finally measured at 734 nm. The antioxidant ability of the samples was calculated based on a reference curve with Trolox and the final antioxidant content was expressed in mg Trolox per mL.

## 2.8. Statistical Analysis

Statistical analysis, including one-way ANOVA, was performed for all datasets using the software TIBCO STATISTICA© (v.13.6.0, TIBCO Software Inc., Palo Alt, CA, USA).

## 3. Results

### 3.1. Morphological Description of the Strains

The LM and TEM images of the strains isolated and studied herein are presented in Figures 2–5. The strain codes were generated using the first three letters of the origin lagoon, the sample they were isolated from, and the order of isolation (e.g., strain KSI 1-3 is the third strain isolated from the first sample taken from the Ksirolimni Lagoon).

- AthU-AI PLA 1-2

Origin: Porto Lagos Lagoon, Macedonia–Thrace, northern Greece.

Isolation date: October 2020

Isolators: X. Chantzistroutsiou Ph.D., A. Ntzouvaras MSc

Preservation salinity: 40‰

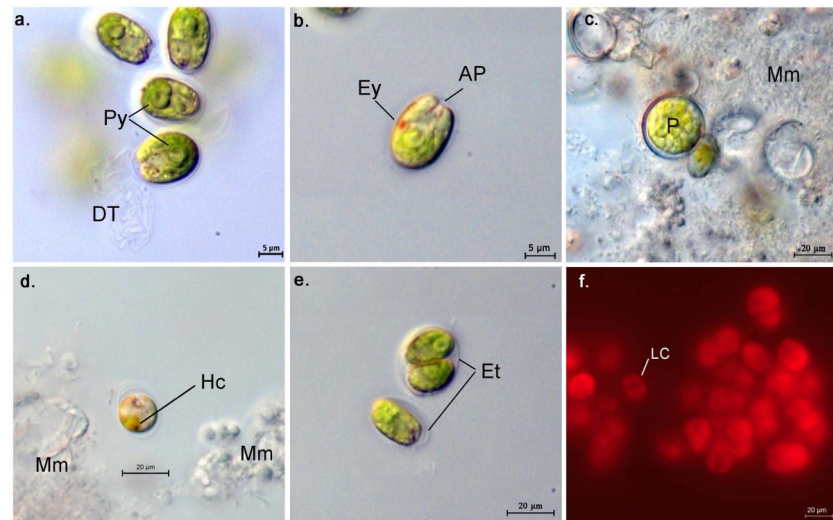


**Figure 2.** Light micrographs of the strain *Tetraselmis* PLA 1-2. (a,b) Living, young cells (post-exponential phase, day 4); (c,d) older cells (advanced stationary phase, day 10); (e) cells during and after division; (f) epifluorescence microscopy photograph showing the chloroplast shape of the cells. Py: pyrenoid; DT: discarded thecae; Ey: eyespot; AP: apical pit; P: palmelloid cell; Mm: mucilaginous material; Hc: hematochrome; Et: external theca; LC: lobed chloroplast. Scale bars: (a,b) = 10 μm, (c–f) = 20 μm.

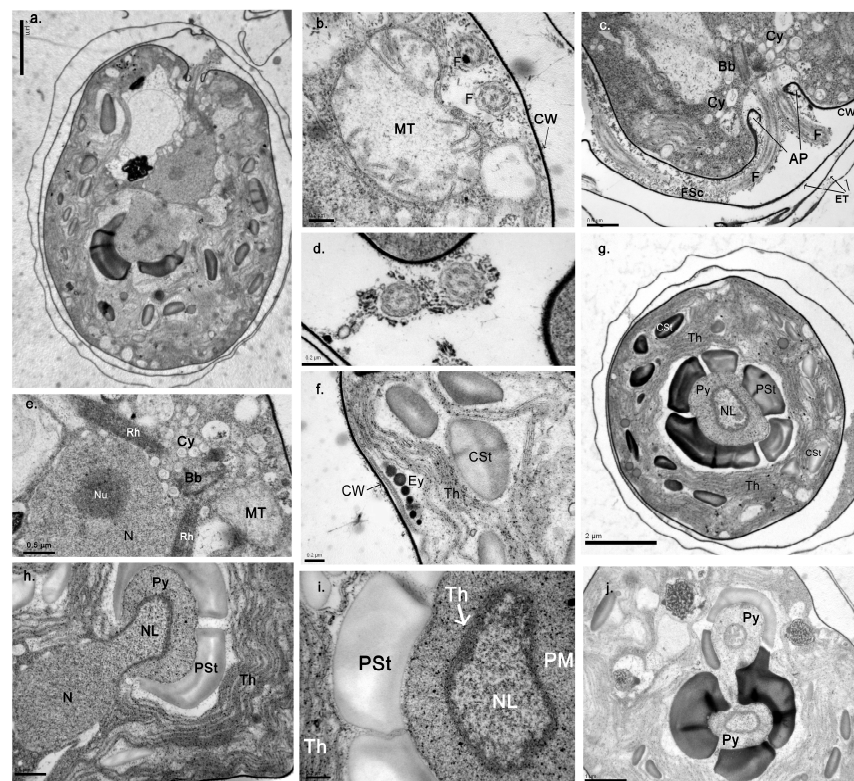


**Figure 3.** Transmission electron micrographs of the strain *Tetraselmis* PLA 1-2. (a) Longitudinal view



of a whole cell; (b,c) details of the anterior part of the cell, longitudinal sections; (d) cross-section of two flagellae; (e) close-up view of the sub-apical part of the cell; (f) detail of the chloroplast; (g) cross-section of the posterior part of the cell; (h) longitudinal view of the pyrenoid area where a lobe of the nucleus can be seen penetrating the pyrenoid; (i) close-up detail of the pyrenoid in the cross-section; (j) cross-section of the posterior part of a cell bearing two pyrenoids. AP: apical pit; F: flagellum; FSc: flagellar scales; CW: cell wall; Bb: basal body; Cy: cysts bearing organic scales; ET: external theca; MT: mitochondrion; Rh: rhizoplast; N: nucleus; Nu: nucleolus; Py: pyrenoid; PSt: pyrenoid sheath starch grain; NL: nucleus lobe; Th: thylacoid membranes; CSt: chloroplast starch grains; Ey: eyespot; PM: pyrenoid matrix. Scale bars: (e,j) = 2  $\mu\text{m}$ , (h) = 1  $\mu\text{m}$ , (a,c,g) = 0.5  $\mu\text{m}$ , (b,d,f,i) = 0.2  $\mu\text{m}$ .

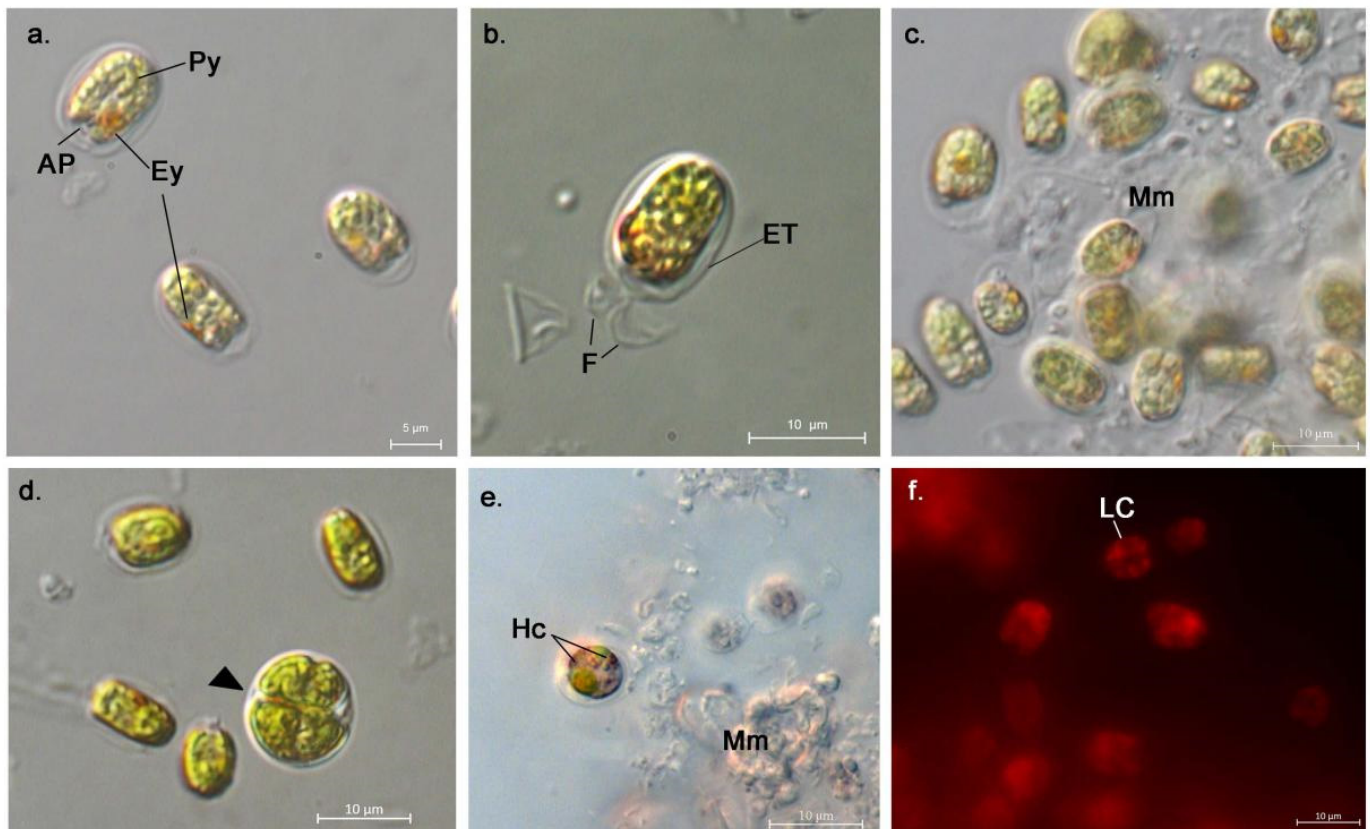


**Figure 4.** Light micrographs of the strain *Tetraselmis* KSI 1-3: (a–d) living, young cells (post-exponential phase, day 4); (e) older cell (advanced stationary phase, day 10); (f) epifluorescence microscopy photograph showing the chloroplast shape of the cells. Py: pyrenoid; Ey: eyespot; AP: apical pit; ET: external theca; F: flagellum; Mm: mucilaginous material; Hc: hematochrome; LC: lobed chloroplast; arrow head: dividing cells. Scale bars: (a) = 5  $\mu\text{m}$ , (b–f) = 10  $\mu\text{m}$ .

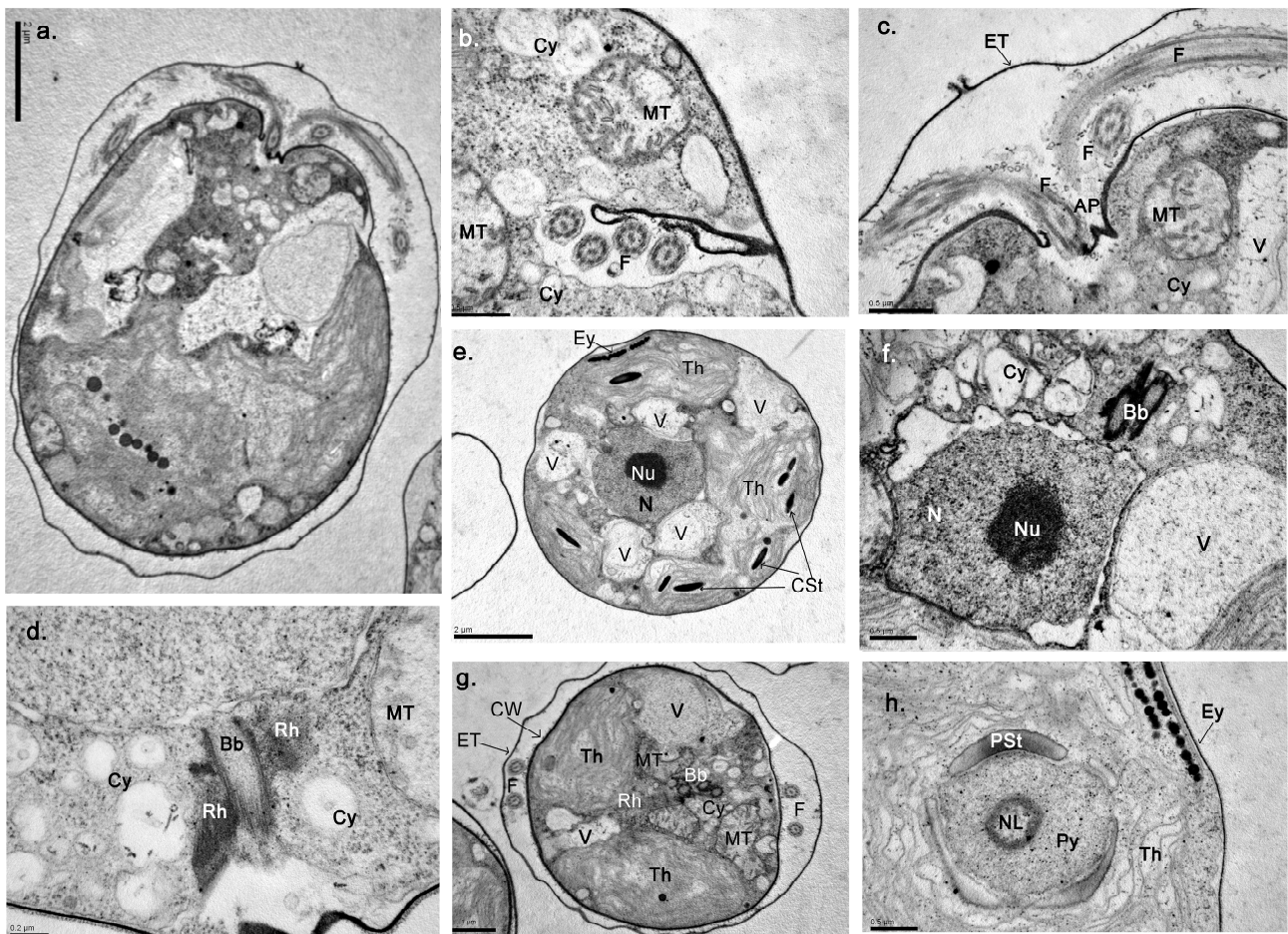


**Figure 5.** Transmission electron micrographs of the strain *Tetraselmis* KSI 1-2. (a) Longitudinal view of a whole cell; (b–d) details of the anterior part of the cell, longitudinal sections; (e) cross-section of the middle part of the cell (whole cell view); (f) close-up cross-section of the anterior part of the cell; (g) cross-section of the anterior part of a whole cell; (h) detail of the chloroplast. AP: apical pit; F: flagellum; ET: external theca; MT: mitochondrion; Cy: cysts bearing organic scales; V: large vacuole; Bb: basal body; Rh: rhizoplast; N: nucleus; Nu: nucleolus; Th: thylacoid membranes; Ey: eyespot; CSt: chloroplast starch grains; Py: pyrenoid; PSt: pyrenoid sheath starch grain; NL: nucleus lobe; CW: cell wall. Scale bars: (e,h) = 2  $\mu\text{m}$ , (g) = 1  $\mu\text{m}$ , (a,b,d,f) = 0.5  $\mu\text{m}$ , (c) = 0.2  $\mu\text{m}$ .

**Morphological description:** The strain presents typical morphological features of the genus *Tetraselmis* Stein (Figures 2 and 3). Cells are ovoid to oblong, rounded or slightly acute posteriorly, approximately 8  $\mu\text{m}$  long and 5  $\mu\text{m}$  wide, and are sheathed within a thin cell wall layer. In motile cells, this layer is usually tightly attached to the cell; however, some cells seem to be enclosed within a rounded theca, including their flagellae (Figures 2e and 3c). Dividing cells and groups of two to four cells resulting from cell division were also enclosed within this round theca prior to being released in the medium in a motile, flagellated form (Figure 2e). Occasionally, the excretion of thecae in a stalk-like manner was observed, as well as the formation of mucilaginous material resulting from the accumulation of excreted thecae (Figure 2c,d). The anterior cavity (apical pit), which is characteristic for the genus, was also observed in LM (Figure 2b) and TEM (Figure 3c), with four (4) flagellae shorter than the cell body emerging from it. In cross-sections, the typical 9 + 2 microtubule formation of the flagellum can be observed (Figure 3d). The flagellar pit seems to bear very few exterior hair-like appendages (flagellar “hairs”) (Figure 3c). The flagellae seem to be emerging from two basal bodies and are located right underneath the apical pit (Figure 3c,e), directly connected with two rhizoplast fibrils which seem to extend towards the periphery of the cell (Figure 3e). Some of the cells appear to exhibit high

metabolic activity in the area right under the flagellar pit, with a plethora of cysts bearing what appears to be cell wall and flagellar coat material (i.e., organic scales), indicating intense dictyosome activity (Figure 3c,e). Additionally, mitochondria are clearly distinct around the area (Figure 3b,e). The chloroplast takes up the greatest part of the cell, and it appears to be massive posteriorly and multi-lobed anteriorly (Figure 2f). The cells appear to have a verrucose (“warty”) texture in LM, indicating the presence of starch grains within the chloroplast stroma; this is verified in the TEM sections where several convex and biconvex starch grains are observed (Figure 3g–f). In LM, cells appear green, with the eyespot not always conspicuous (Figure 2b); the eyespot is usually located peripherally within the cell or close to the pyrenoid, in the form of lipid granules in TEM (Figure 3f). A large, sub-central pyrenoid is observed, which may appear U-shaped under LM (Figure 2a); this is due to the fact that a large lobe of the nucleus penetrates the pyrenoid (Figure 3h–i). The nuclear material is separated from the pyrenoid matrix by a thin layer of thylacoid membrane (Figure 3i). The pyrenoid is surrounded by a sheath of plano-concave starch grains which appear to be larger and thicker than those of the chloroplast stroma (Figure 3g). It is important to note that in the TEM sections, some cells appeared to have two pyrenoids connected to each other, each penetrated by a lobe of the nucleus and each having their own starch sheath (Figure 3j). The nucleus is located centrally within the cell, between the pyrenoid and the basal bodies, and bears a distinct nucleolus (Figure 3e). In older cultures (stationary phase), palmelloid cells were also observed, i.e., round, immotile cells larger than the regular cells with a thick cell wall (Figure 2c). Some cells appear to have orange-red pigmentation on the anterior part of the cells (not associated with the eyespot), indicating the accumulation of what is referred to as “hematochrome” (Figure 2d) by Norris et al. [16]. The macroscopic view of the strain cultures presents an interesting image, as it has a green coloration during the first stages of growth (up to the post-exponential phase) that gradually turns dark red during senescence (stationary phase) (Figure 6).

- AthU-AI KSI 1-3

Origin: Ksirolimni Lagoon, Thrace, northern Greece.

Isolation date: October 2020

Isolators: X. Chantzistroutsiou PhD, A. Ntzouvaras MSc

Preservation salinity: 40‰

Morphological description: This strain also presents typical morphological features of the genus *Tetraselmis* Stein (Figures 4 and 5), as described before for strain PLA 1-2, with certain variations. The cells size seems to be slightly larger (~9 µm long and ~6 µm wide). The anterior cavity (apical pit) seems to bear far fewer, if any, flagellar “hairs” exteriorly compared to PLA 1-2 (Figure 5c). The eyespot is much larger and more clearly distinct in LM (Figure 4a). The chloroplast stroma bears far fewer starch grains, which are smaller and less thick than those of the previous strain, while the pyrenoid sheath starch grains seem to also be plano-concave (Figure 5h). The dictyosome activity is intense in this case as well, and rather large vacuoles were observed surrounding the nucleus in most cells (Figure 5e). In this strain, no cells were observed bearing more than one pyrenoid. Additionally, no palmelloid cells were observed in older cultures. The macroscopic view of the strain culture presents the same image (Figure 6) as before, and the accumulation of “hematochrome” (Figure 4e) is present in the cells as well.

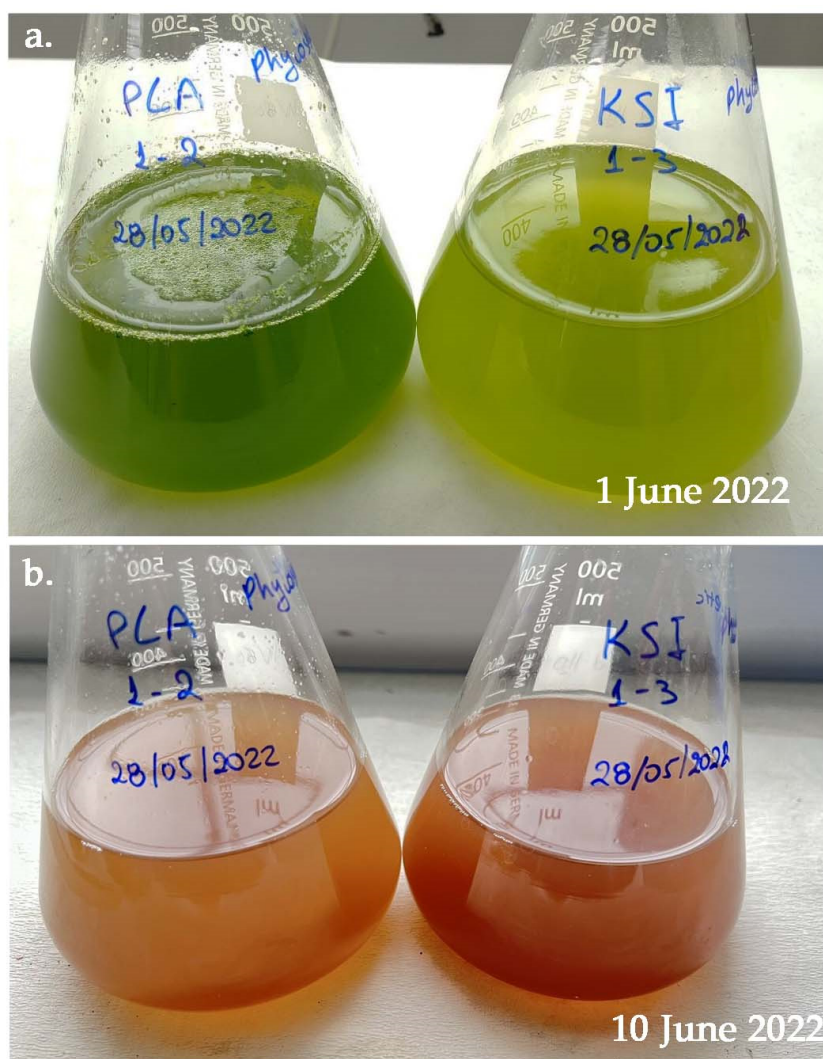


**Figure 6.** Macroscopic image of liquid cultures of the strains PLA 1-2 and KSI 1-3. (a) Fresh culture (post-exponential phase, day 5); (b) older culture (advanced stationary phase, day 15).

Based on the morphological features of the cell and the available systematic keys for the genus *Tetraselmis* [16,17], the taxonomic classification for both strains is as follows [38]:

Kingdom: Plantae  
 Subkingdom: Viridiplantae  
 Phylum: Chlorophyta  
 Class: Chlorodendrophyceae  
 Order: Chlorodendrales  
 Family: Chlorodentraceae  
 Genus: *Tetraselmis* Stein 1878  
 Subgenus: *Prasinocladia*  
 Species: *Tetraselmis verrucosa* Butcher, 1956  
 Subspecies/form: *Tetraselmis verrucosa* f. *rubens* Hori, Norris, and Chihara, 1983

### 3.2. Molecular Analyses

A summary of the results from the BLAST search of the strain genes is presented in Table 3. The presented results were selected based on percentage (%) identity and an E-value of 0 since those are the ones that are more likely to reflect genus- and species-level similarities. The complete sequences generated for the selected genes can be found in Supplemental File S2. Both strains showed great similarity based on the *rbcL* gene (~97%)

with the taxon *Tetraselmis rubens*, which is currently regarded as a synonym for *Tetraselmis verrucosa* f. *rubens* [38]. Additionally, based on the 18S gene, the strain KSI 1-3 showed 99.81% similarity with several isolates of the taxon *T. rubens*. Based on *ITS* sequences, both strains showed ~99.7% similarity with the strain *Tetraselmis* sp. DS3, which has not been identified further than the genus level. Additionally, the strains showed similarities with the species *T. marina* based on the *tufA* sequences.

**Table 3.** Summary of selected BLAST results for the identification of the strains according to the generated genetic sequences.

Genetic Locus	Strain Code	Accession Number	Score (Bits)	Identities (ID)	% ID	Gaps	Strand	Scientific Name
<i>ITS</i>	PLA 1-2	KP100529.1	1101	599/601	99.67	0	++	<i>Tetraselmis</i> sp. DS3
	KSI 1-3		1101	599/601	99.67	0	++	
<i>rbcL</i>	PLA 1-2	KX904699.1	1042	600/618	97.09	0	++	<i>Tetraselmis rubens</i> V 2_2
	KSI 1-3		941	541/558	96.95	0	++	
<i>tufA</i>	PLA 1-2	ON645926.1	1149	824/924	89.18	3/924	++	<i>Tetraselmis marina</i>
	KSI 1-3		1171	838/939	89.24	3/939	+−	
18S	KSI 1-3 data	OQ220342.1	2974	1615/1618	99.81	1/1618	++	<i>Tetraselmis marina</i> BEA0158B
		KX904704.1	2916	1584/1587	99.81	1/1587	++	<i>Tetraselmis rubens</i> R 9_3
		KX904703.1	2913	1582/1585	99.81	1/1585	++	<i>Tetraselmis rubens</i> R 9_2
		KT860871.1	2876	1562/1565	99.81	1/1565	++	<i>Tetraselmis rubens</i> RCC133

The sequences generated for the *rbcL* and *tufA* genes were additionally used for the generation of a concatenated phylogenetic tree (Figure 7). The two strains were very strongly grouped together with a bootstrap value of 100% and were also grouped with several other *Tetraselmis* sp. strains; however, the tree is not resolved, and therefore more data are required in order to draw safe conclusions on the strains' phylogenetic positions. It should be noted that no sequences of the *tufA* or *ITS* genes were available in the GenBank database for the species *T. verrucosa*, and a large number of the sequences for the *Tetraselmis* genus were not identified at the species level for all genetic loci. Additionally, the same sequence seemed to have been submitted more than once with different accession numbers in some cases; therefore, they showed up as different entries. Some of the sequences used for the generation of the tree belong to other *Tetraselmis* strains isolated by the authors and the data have not been published; the sequences can be found in Supplemental File S2, along with a full list of the accession numbers of the taxa used for the molecular analyses.

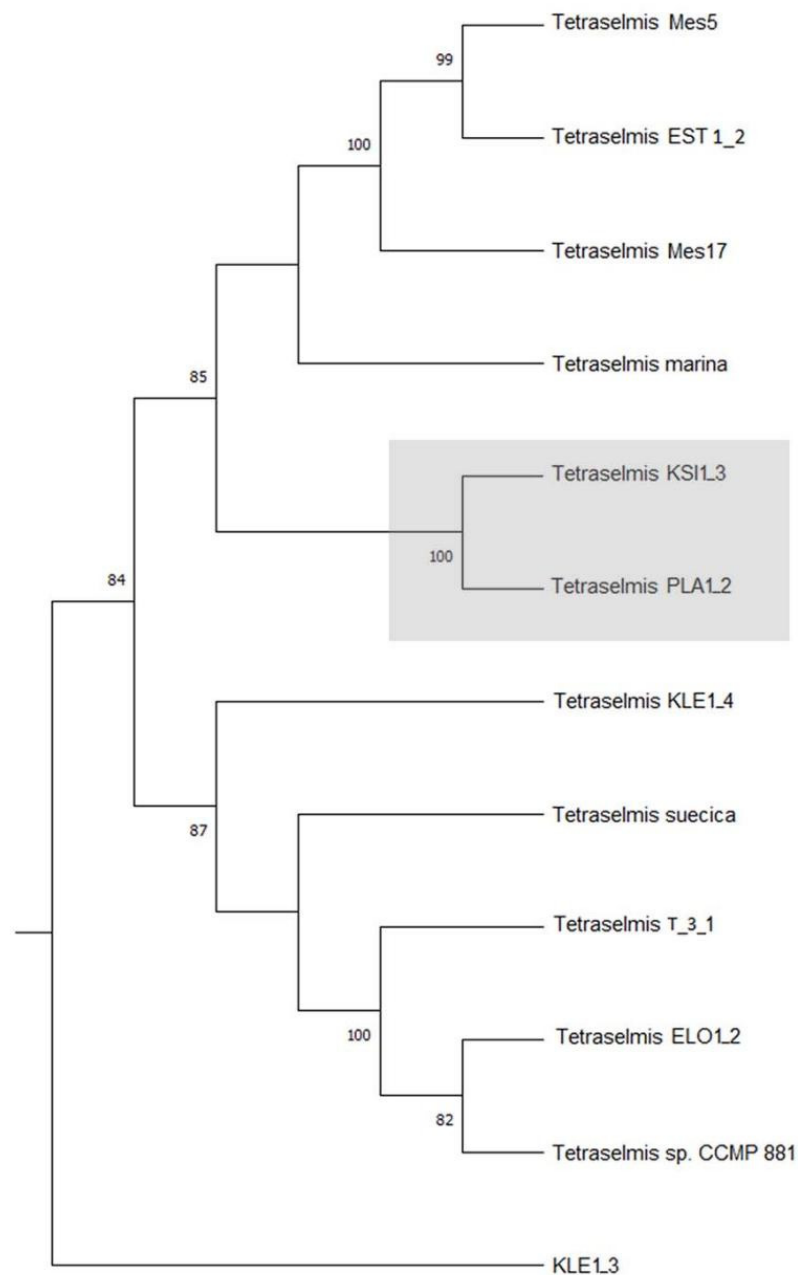


**Figure 7.** Consensus tree inferred with MrBayes based on *rbcL* and *tufA* genetic sequences. Numbers on the nodes correspond to bootstrap values, indicating the percentage of similarity between the linked sequences. The strains *Tetraselmis* KSI 1-3 and *Tetraselmis* PLA 1-2 studied herein have been identified as representatives of *Tetraselmis verrucosa f. rubens*.

These results corroborate the findings of the morphological identification of the strains, placing them within the species *T. verrucosa f. rubens*.

### 3.3. Culture Kinetics

Growth kinetics data of the strains cultivated in the same conditions are shown in Figure 8. The strain PLA 1-2 showed a higher growth rate ( $\mu$ ) and higher cell density, especially during the post-exponential and stationary phases when algal culture typically reaches highest yield (i.e., the net number of cells produced). More specifically, PLA 1-2 reached a  $\mu_{\max}$  of  $0.8 \pm 0.06 \text{ d}^{-1}$ , while KSI 1-3 reached a  $\mu_{\max}$  of  $0.6 \pm 0.05 \text{ d}^{-1}$ . Both strains reached the stationary phase on day 5 and growth rates started declining from then on, while cell productivity was relatively stabilized at around  $1.8 \times 10^5 \text{ cells} \cdot \text{mL}^{-1} \cdot \text{day}^{-1}$ .

for PLA 1-2 and  $1.4 \times 10^5$  cells·mL<sup>-1</sup>·day<sup>-1</sup> for KSI 1-3. However, KSI 1-3 reached higher values in terms of biomass production, i.e., dry weight ( $\sim 1.53 \pm 0.06$  g·L<sup>-1</sup>), than PLA 1-2 ( $1.13 \pm 0.03$  g·L<sup>-1</sup>); this could be due to the larger mean cell size of the KSI 1-3 strain. The mean cell biovolume was  $169.60 \pm 0.16$   $\mu\text{m}^3$ ·cell<sup>-1</sup> for PLA 1-2 and  $276.91 \pm 0.24$   $\mu\text{m}^3$ ·cell<sup>-1</sup> for KSI 1-3.

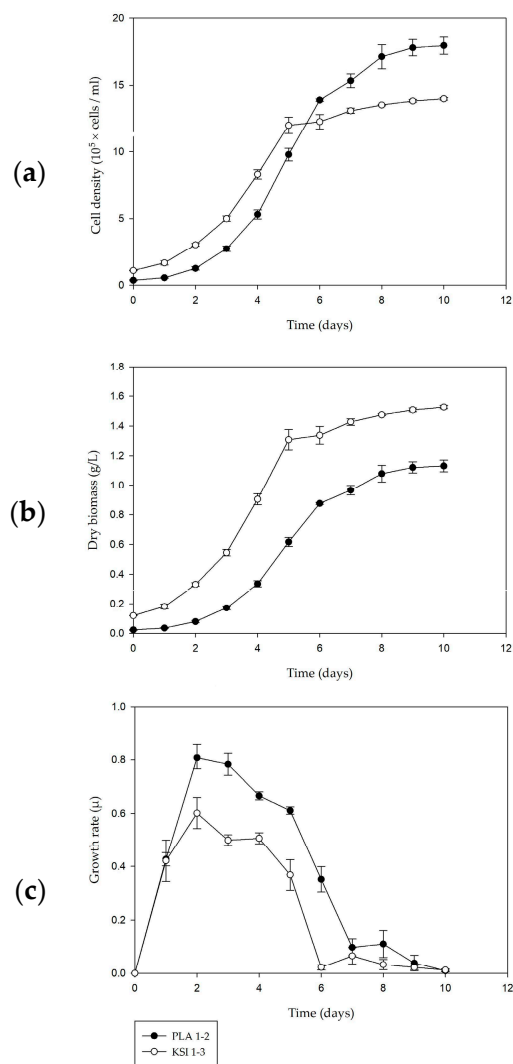


**Figure 8.** Growth kinetics of the studied strains: (a) daily cell productivity (cells·mL<sup>-1</sup>); (b) daily biomass production (g·L<sup>-1</sup>); (c) growth rate ( $\mu$ , d<sup>-1</sup>). Values are the average of ( $n = 3$ ) three replicates; standard error is shown with error bars.

### 3.4. Biochemical Analyses

The biochemical composition of the studied strains is shown in Table 4.

**Table 4.** Biochemical composition data of the strains PLA 1-2 and KSI 1-3. Sampling for all analyses was performed on day 10.

Strain	Chl <i>a</i> (mg/g DW)	Chl <i>b</i> (mg/g DW)	TC (mg/g DW)	TP (% of DW)	TL (% of DW)	PS (% of DW)
PLA 1-2	7.58 ** $\pm$ 0.54	5.73 ** $\pm$ 0.48	3.25 * $\pm$ 0.25	15.76 * $\pm$ 1.09	16.37 * $\pm$ 0.98	40.94 ** $\pm$ 1.71
KSI 1-3	5.16 ** $\pm$ 0.17	3.46 ** $\pm$ 0.15	3.71 * $\pm$ 0.12	28.60 * $\pm$ 1.35	12.77 * $\pm$ 1.25	27.76 ** $\pm$ 0.03

Note(s): Chl *a*: chlorophyll *a*; Chl *b*: chlorophyll *b*; TC: total carotenoids; TP: total protein; TL: total lipids; PS: total polysaccharides; DW: dry weight. Values are shown as the average of ( $n = 3$ ) three replicates  $\pm$  standard error (statistically significant differences: \*  $p < 0.05$ , \*\*  $p < 0.01$ ).

Both strains exhibited relatively high polysaccharide content, especially PLA 1-2 (40.94%); PS content for the genus *Tetraselmis* is usually found to be around 8–12% [39,40], although higher values (45%) have been reported [7]. Protein content is higher for the strain KSI 1-3 (28.60%) compared to PLA 1-2 (15.76%) and close to the average previously reported for the genus *Tetraselmis* [39–41], while total lipid content (~13–16%) is also average up to high for both strains compared to previously reported values [7,39–41]. Pigment values are as expected, although they were higher for PLA 1-2 compared to KSI 1-3; these findings are also in agreement with previously reported values [42]. It should be noted that the strains were cultivated under favorable conditions (no stress or optimization regimes were applied for the enhancement of metabolite production).

### 3.5. Antioxidant Capacity

The results of the antioxidant capacity assays for the strains are summarized in Table 5.

**Table 5.** Summary of antioxidant capacity assays for the strains PLA 1-2 and KSI 1-3. Sampling for all analyses was performed on day 10.

Strain	TPC (mg Gallic Acid/g DW)	TFC (mg Quercetin/g DW)	FRAP (mg Ascorbic Acid/g DW)	TEAC (mg TROLOX/g DW)
PLA 1-2	5.99 ± 0.09	1.34 ** ± 0.11	1.42 ** ± 0.02	3.73 ** ± 0.37
KSI 1-3	5.84 ± 0.05	3.77 ** ± 0.32	1.70 ** ± 0.03	5.49 ** ± 0.09

Note(s): TPC: total phenolic content; TFC: total flavonoid content; FRAP: Ferric Reducing Antioxidant Power; TEAC: Trolox Equivalent Antioxidant Capacity; DW: dry weight. Values are shown as the average of ( $n = 3$ ) three replicates ± standard error (statistically significant differences: \*\*  $p < 0.01$ ).

Both strains used in this study exhibited similar phenolic content; however, the strain KSI 1-3 exhibited significantly higher flavonoid content than PLA 1-2, which was almost threefold higher (3.77 and 1.34 mg gallic acid/g DW, respectively). Both strains scored better in the TEAC treatment than they did in FRAP, with KSI 1-3 showing higher values in this case as well.

## 4. Discussion

The discovery, thorough identification, and investigation of novel microalgal strains is a timely and viable prospect for both international and local industries. Furthermore, the isolation and identification of local strains with biotechnological potential can contribute to the sustainable development of local industries, exploiting the natural wealth and biodiversity of each area. The present study is oriented towards this perspective.

Both strains described herein have been identified as representatives of the taxon *Tetraselmis verrucosa* f. *rubens* (Butcher) Hori, Norris, and Chihara [17] according to morphological and molecular criteria. Strains of this taxon have been recorded in several other transient systems of Greece in the past few decades, including the lagoons of Rhodia and Vatatsa in Epirus and the lagoonal system of Messolonghi in Aetoloakarnania, western Greece [5]. The two strains presented here are the first representatives of the taxon recorded for northern Greece, while the species has also appeared in samples taken from other lagoons in both western and northern Greece. *Tetraselmis* is among the most common genera in aquatic systems with representatives within the whole range of such environments, including freshwater, oceanic, transitional, and hypersaline habitats [43]. Additionally, the taxonomic position of the species belonging to the genus *Tetraselmis* has undergone several revisions through the decades. This genus was traditionally placed within the paraphyletic class of Prasinophyceae; however, with the rise of molecular phylogenetic data, it was placed in a new class, Chlorodendrophyceae, which appears to be a phylogenetic link between true prasinophytes and chlorophytes, though the evolutionary relationship among the clades is yet to be elucidated [8]. Despite its great importance, there are very few phylogenetic studies focusing on the genus [5,44,45], and the most detailed morphological studies



are the ones presented by Hori et al. [17,46,47]. The aforementioned authors performed extensive ultrastructural TEM studies on a plethora of the genus representatives and placed the then known species within four subgenera: *Tetraselmis*, *Prasinocladia*, *Tetrathele*, and *Parviselmis*. The two studied strains were placed within the subgenus *Prasinocladia* based on morphological features of the pyrenoid, the apical pit, and the microscopic and macroscopic image of the cultures (accumulation of hematochrome within the cells and red coloration of the culture medium). However, in this study, a novel feature has been revealed in the cell ultrastructure: the presence of more than one pyrenoid within the chloroplast was detected in strain PLA 1-2. This observation does not only differentiate the two strains more radically than any other difference noticed between them, but it also raises questions about the credibility of the pyrenoid structure as a species-defining characteristic within the genus, which has been noted previously [45]. The presence of more pyrenoids within cells of the species has been previously hinted, but it was considered as an LM observation artifact since it had not been verified through ultrastructural data [5]. However, in light of the results presented in this study, the presence of more than one pyrenoid within some of the cells of the species is indubitable as it has been observed in both LM and TEM images. This can give rise to further investigation of the morphological criteria used to define species and below-species level classification within the genus. Moreover, it has become apparent that morphology alone is not sufficient for the conclusive identification of microalgal strains, and the need for comparative analysis of molecular and morphological data is more present than ever [5,8,48]. The molecular data resulting from this study support the morphological identification of the strains; however, the phylogenetic analysis and classification is lacking, as there are very few available sequences for the taxon submitted in GenBank. Moreover, there are also few available sequences for the genus *Tetraselmis* in general, especially for the *tufA* gene, which has been previously used successfully for assessment of the phylogenetic position and relationships of microalgae [23,49].

Regarding biokinetic data, the studied strains show comparable growth rates (when cultivated under relatively similar culture conditions) with other *Tetraselmis* strains (e.g., [4,50,51]). While both studied strains demonstrated cell densities lower than those reported for other *Tetraselmis* strains, they also demonstrated considerably higher growth rates and biomass production [52–56]. These results could be explained by the relatively large biovolume of both studied strains, as well as the favorable conditions applied during their cultivation in order to simulate those of the original habitats. This method can minimize the applied stress, enabling enhanced growth and productivity. Although culture kinetics is heavily influenced by the culture conditions of the strain, these results are indicative of the strains' potential for mass cultivation.

The gross biochemical composition of the strains studied in this research is more or less in agreement with other reports for the genus *Tetraselmis* [39,40,55]. It is noteworthy, however, that the polysaccharide content of the strains presented herein is rather high compared to most reports, especially in case of PLA 1-2 (PS ~41% of DW), which presented one of the highest content values in the literature, making it a potential polysaccharide producer. The strain *Tetraselmis* sp. BPE14 reported by Barten et al. [41] exhibited elevated polysaccharide content very similar to that of the studied strains. The lipid content of the strains is also higher than in most reports (e.g., [7,39–41]). It is noteworthy that no methods for triggering lipid accumulation were used in the framework of the present study; with the use of such techniques (e.g., nitrate depletion) *Tetraselmis* strains can reach total lipids values of up to 50% [57,58]. Moreover, *Tetraselmis* has been shown to produce high-value fatty acids such as EPA (eicosapentaenoic acid) [4,5,59,60]. It should be noted that cultivation conditions and the synthesis of the culture medium used can cause significant changes in the biochemical composition of the strains. The lipid content of the two studied strains warrants further research regarding their specific fatty acid profile and content, as well as the use of methods that will enhance the production of lipids to allow for their possible exploitation in the food and aquaculture industries.

Chlorophyll *a* and *b* content was within the expected range in both strains and is in agreement with previous reports for the genus [61–63]. Chlorophyll *a* content is affected by various factors, such as light, nutrient concentration, temperature, salinity, and the growth phase [61,62,64], and different cultivation regimes could therefore result in different chlorophyll composition; however, the strain PLA 1-2 demonstrated almost double the values of KSI 1-3, possibly indicating a differentiated response of the photosynthetic mechanism to environmental conditions.

The taxon *Tetraselmis verrucosa* f. *rubens* has not been thoroughly studied despite the various interesting characteristics it possesses, with its high carotenoid content revealed by both morphological and biochemical data being the most prominent characteristic. Carotenoids are pigments used in a wide variety of industries, and finding strains with high carotenoid content is thus of great importance. The carotenoid content of the species estimated in the framework of this study is rather high, especially considering that no methods for the enhancement or induction of carotenoid production, nor sophisticated carotenoid extraction techniques, were used. Both strains investigated herein demonstrated significant total carotenoid content greater or similar to that reported previously (e.g., [40,42,65]), with strain KSI 1-3 demonstrating slightly higher content compared to PLA 1-2. These results are comparable to the really promising *Tetraselmis* strains studied by Ahmed et al. [42] and Goiris et al. [65].

Furthermore, carotenoids have been shown to have potent antioxidant properties [66,67]. Another important class of antioxidants, well known from terrestrial plants, are phenolic compounds and flavonoids, a large group of complex phenolic compounds [68,69]. The TPC and TFC values in the studied strains are in accordance with previous reports on microalgae [65,70,71]. In order to further assess the antioxidant potential of the studied strains, both FRAP and TEAC methods were deployed; although the results received for TEAC were promising and comparable to previously reported values, the results received for FRAP were relatively poor [70–74]. Although phenolic substances are important antioxidants in terrestrial plants, it remains unclear whether they exhibit equally important activity in microalgae. Many studies have compared phenolic content and antioxidant activity in microalgae, with results yielding both positive (e.g., [75,76]) and negative (e.g., [77]) outcomes. In the present work, two strains and two antioxidant activity measuring methods were used, and it is worth noting that the strain which presented slightly higher carotenoid content and significantly higher flavonoid content (KSI 1-3) was the one that also exhibited higher antioxidant activity.

The results presented herein were received after cultivation under optimal conditions, and the antioxidant capacity measured was therefore not enhanced as there was no stress (oxidative or otherwise) applied to the cells. Moreover, the antioxidant capacity observed is strongly influenced by the extraction method and the selected fraction [78]; therefore, further research should be performed using oxidative stress and different extraction protocols in order to fully explore the antioxidant capacity of the studied strains.

## 5. Conclusions

The ecological significance of microalgae is irrefutable; nevertheless, in the past decades their biotechnological and industrial potential has been intensively studied and exploited in various sections, such as aquaculture, food, pharmaceutical, and cosmetic industries and even nanotechnology. As a result, the need for the discovery and thorough identification and investigation of novel microalgal strains is a current and viable prospect for both international and local industries. Furthermore, the isolation and identification of local strains with biotechnological potential can contribute to the sustainable development of local industries, exploiting the natural wealth and biodiversity of each area. The present study was oriented towards this perspective. Both strains studied here show promising results from a biotechnological aspect due to both their composition and their growth characteristics. However, in order to fully understand their possibilities and to fully exploit their biotechnological potential, further research is needed. This should include methods for

enhancing and inducing the production of secondary metabolites and further assessment of their antioxidant and anti-inflammatory properties.

**Supplementary Materials:** The following supporting information can be downloaded at: <https://www.mdpi.com/article/10.3390/w15091698/s1>, Supplemental File S1: Chemical Composition of Culture Media; Supplemental File S2: Genetic sequences generated from the studied strains.

**Author Contributions:** Conceptualization, I.T., E.F., A.N. and X.C.; methodology, I.T., E.F., I.-D.A., A.K., M.-E.Z., S.M. and G.V.; validation, A.E.-A.; formal analysis, N.P., X.C., A.N., A.K. and A.T.; investigation, N.P., X.C., A.N., A.K., M.-E.Z., S.M. and G.V.; resources, A.E.-A., I.T., I.-D.A. and E.F.; data curation, A.N. and X.C.; writing—original draft preparation, X.C., A.N. and A.T.; writing—review and editing, A.E.-A.; visualization, A.N., X.C., I.-D.A. and A.K.; supervision, A.E.-A.; project administration, A.E.-A. and E.F.; funding acquisition, A.E.-A. and E.F. All authors have read and agreed to the published version of the manuscript.

**Funding:** This research was co-financed by Greece and the European Union (European Regional Development Fund—ERDF) through the Operational Program Competitiveness, Entrepreneurship and Innovation in the context of the project “Phycosmetic-GR” (MIS 5045811).

**Data Availability Statement:** Data are available upon request from the authors.

**Acknowledgments:** The authors would like to express their thanks to Emmanuel Panteris (Department of Biology, Aristotle University of Thessaloniki) for his assistance in obtaining the TEM images and Sophia Papadaki (National Technical University of Athens, School of Chemical Engineering) for her contribution in processing the algal biomass.

**Conflicts of Interest:** The authors declare no conflict of interest. The funders had no role in the design of the study; in the collection, analyses, or interpretation of data; in the writing of the manuscript; or in the decision to publish the results.

## References

- Blackburn, S.I.; Lee-Chang, K.J. Microalgae: A renewable resource for food and fuels and more. In *Blue Biotechnology: Production and Use of Marine Molecules*; La Barre, S., Bates, S.S., Eds.; Wiley-VCH: Weinheim, Germany, 2018; Volume 1, pp. 1–32. [\[CrossRef\]](#)
- Newton, A.; Icely, J.; Cristina, S.; Brito, A.; Cardoso, A.C.; Colijn, F.; Dalla Riva, S.; Gertz, F.; Hansen, J.W.; Holmer, M.; et al. An overview of ecological status, vulnerability and future perspectives of European large shallow, semi-enclosed coastal systems, lagoons and transitional waters. *Estuar. Coast. Shelf Sci.* **2014**, *140*, 95–122. [\[CrossRef\]](#)
- Pérez-Ruzafa, A.; Pérez-Ruzafa, I.M.; Newton, A.; Marcos, C. Coastal lagoons: Environmental variability, ecosystem complexity, and goods and services uniformity. In *Coasts and Estuaries: The Future*; Wolanski, E., Day, J.W., Elliott, M., Ramachandran, R., Eds.; Elsevier: Amsterdam, The Netherlands, 2019; pp. 253–276. [\[CrossRef\]](#)
- Tzovenis, I.; Fountoulaki, E.; Dolapsakis, N.; Kotzamanis, I.; Nengas, I.; Bitis, I.; Cladas, Y.; Economou-Amilli, A. Screening for marine nanoplanktic microalgae from Greek coastal lagoons (Ionian Sea) for use in mariculture. *J. Appl. Phycol.* **2009**, *21*, 457–469. [\[CrossRef\]](#)
- Chantzistroutsou, X.; Tzovenis, I.; Parmakellis, A.; Economou-Amilli, A. Characterization of *Tetraselmis verrucosa* f. *rubens* (Chlorodendrophyceae) strains from coastal lagoons of Western Greece using a multivariate approach. *Phytotaxa* **2016**, *278*, 225–240. [\[CrossRef\]](#)
- Qazi, W.M.; Ballance, S.; Uhlen, A.K.; Kousoulaki, K.; Haugen, J.E.; Rieder, A. Protein enrichment of wheat bread with the marine green microalgae *Tetraselmis chuii*—Impact on dough rheology and bread quality. *LWT* **2021**, *143*, 111115. [\[CrossRef\]](#)
- Schüler, L.M.; Bombo, G.; Duarte, P.; Santos, T.F.; Maia, I.B.; Pinheiro, F.; Marques, J.; Jacinto, R.; Schulze, P.S.; Pereira, H.; et al. Carotenoid biosynthetic gene expression, pigment and n-3 fatty acid contents in carotenoid-rich *Tetraselmis striata* CTP4 strains under heat stress combined with high light. *Bioresour. Technol.* **2021**, *337*, 125385. [\[CrossRef\]](#)
- Leliaert, F.; Smith, D.R.; Moreau, H.; Herron, M.D.; Verbruggen, H.; Delwiche, C.F.; De Clerck, O. Phylogeny and molecular evolution of the green algae. *Crit. Rev. Plant. Sci.* **2012**, *31*, 1–46. [\[CrossRef\]](#)
- Efthimiou, G.; Mertzanis, A.; Emmanouloudis, D. Direct and indirect human-made impact on the natural ecosystems of the River Nestos. In Proceedings of the First International Conference on Environmental Research and Assessment, Ars Docenti, Romania, 23–27 March 2003; pp. 23–27.
- Dafis, S.; Papastergiadou, E.; Georgiou, K.; Babalonas, D.; Georgiadis, T.; Papageorgiou, M.; Lazaridou, T.; Tsiaousi, V. (Eds.) *Directive 92/43/EC Works Biotopes in Greece: Network Natura 2000*; Gouladri Museum of Natural History—Hellenic Center of Biotopes and Wetlands, EKBY: Thessaloniki, Greece, 1997.
- Pavlikakis, G.E.; Tsihrintzis, V.A. Integrating humans in ecosystem management using multi-criteria decision making. *J. Am. Water Resour. Assoc.* **2003**, *39*, 277–288. [\[CrossRef\]](#)

12. Municipality of Komotini Official Website. Available online: <https://www.komotini.gr/perivalon/fysiko-perivallon> (accessed on 3 March 2023). (In Greek).
13. NaturaGraeca, Nestos Delta and Lakes Vistonida-Ismarida. Available online: <https://www.naturagraeca.com/ws/119,181,385,2,1,Nestos-Delta-and-lakes-Vistonida-Ismarida> (accessed on 3 March 2023).
14. Guillard, R.R.L.; Hargraves, P.E. *Stichochrysis immobilis* is a diatom, not a chrysophyte. *Phycologia* **1993**, *32*, 234–236. [[CrossRef](#)]
15. Andersen, R.A.; Kawachi, M. Traditional Microalgae Isolation Techniques. In *Algal Culturing Techniques*; Andersen, R.A., Ed.; Elsevier Academic Press: Oxford, UK, 2005; pp. 90–92.
16. Norris, R.E.; Hori, T.; Chihara, M. Revision of the genus *Tetraselmis* (class Prasinophyceae). *Bot. Mag.* **1980**, *93*, 317–339. [[CrossRef](#)]
17. Hori, T.; Norris, R.E.; Chihara, M. Studies on the ultrastructure and taxonomy of the genus *Tetraselmis* (Prasinophyceae). II: Subgenus *Prasinocladia*. *Bot. Mag.* **1983**, *96*, 385–392. [[CrossRef](#)]
18. Hillebrand, H.; Dürselen, C.D.; Kirschtel, D.; Pollinger, U.; Zohary, T. Biovolume calculation for pelagic and benthic microalgae. *J. Phycol.* **1999**, *35*, 403–424. [[CrossRef](#)]
19. Olmos-Soto, J.; Paniagua-Michel, J.; Contreras, R.; Ochoa, L. DNA Fingerprinting Intron-Sizing Method to Accomplish a Specific, Rapid, and Sensitive Identification of Carotenogenic *Dunaliella* Species. In *Microbial Carotenoids from Bacteria and Microalgae*; Barredo, J.L., Ed.; Humana Press: Totowa, NJ, USA, 2012; Volume 892, pp. 269–281. [[CrossRef](#)]
20. Nozaki, H.; Itoh, M.; Sano, R.; Uchida, H.; Watanabe, M.M.; Kuroiwa, T. Phylogenetic relationships within the colonial Volvocales (Chlorophyta) inferred from *rbcl* gene sequence data. *J. Phycol.* **1995**, *31*, 970–979. [[CrossRef](#)]
21. Assunção, P.; Jaén-Molina, R.; Caujapé-Castells, J.; de la Jara, A.; Carmona, L.; Freijanes, K.; Mendoza, H. Phylogenetic position of *Dunaliella acidophila* (Chlorophyceae) based on ITS and *rbcl* sequences. *J. Appl. Phycol.* **2012**, *24*, 635–639. [[CrossRef](#)]
22. Preetha, K.; John, L.; Subin, C.S.; Vijayan, K.K. Phenotypic and genetic characterization of *Dunaliella* (Chlorophyta) from Indian salinas and their diversity. *Aquat. Biosyst.* **2012**, *8*, 27. [[CrossRef](#)]
23. Vieira, H.H.; Bagatini, I.L.; Guinart, C.M.; Vieira, A.A.H. *tufA* gene as molecular marker for freshwater Chlorophyceae. *Algae* **2016**, *31*, 155–165. [[CrossRef](#)]
24. Clark, K.; Karsch-Mizrachi, I.; Lipman, D.J.; Ostell, J.; Sayers, E.W. GenBank. *Nucleic Acids Res.* **2016**, *44*, D67–D72. [[CrossRef](#)]
25. Kumar, S.; Stecher, G.; Li, M.; Niyaz, C.; Tamura, K. MEGA X: Molecular Evolutionary Genetics Analysis across Computing Platforms. *Mol. Biol. Evol.* **2018**, *35*, 1547–1549. [[CrossRef](#)] [[PubMed](#)]
26. Nei, M.; Kumar, S. *Molecular Evolution and Phylogenetics*; Oxford University Press: New York, NY, USA, 2000; ISBN 0-19-513584-9.
27. Kimura, M. A simple method for estimating evolutionary rates of base substitutions through comparative studies of nucleotide sequences. *J. Mol. Evol.* **1980**, *16*, 111–120. [[CrossRef](#)]
28. Bremner, J.M. Total nitrogen. In *Methods of Soil Analysis: Part 2 Chemical and Microbiological Properties 9.2*; Norman, A.G., Ed.; American Society of Agronomy: Madison, WI, USA, 1965; pp. 1149–1178. [[CrossRef](#)]
29. Olsen, M.F.L.; Pedersen, J.S.; Thomsen, S.T.; Martens, H.J.; Petersen, A.; Jensen, P.E. Outdoor cultivation of a novel isolate of the microalgae *Scenedesmus* sp. and the evaluation of its potential as a novel protein crop. *Physiol. Plant.* **2021**, *173*, 483–494. [[CrossRef](#)]
30. Mishra, S.K.; Suh, W.I.; Farooq, W.; Moon, M.; Shrivastav, A.; Park, M.S.; Yang, J.W. Rapid quantification of microalgal lipids in aqueous medium by a simple colorimetric method. *Biores. Tech.* **2014**, *155*, 330–333. [[CrossRef](#)]
31. DuBois, M.; Gilles, K.A.; Hamilton, J.K.; Rebers, P.T.; Smith, F. Colorimetric method for determination of sugars and related substances. *Anal. Chem.* **1956**, *28*, 350–356. [[CrossRef](#)]
32. Borovkov, A.B.; Gudvilovich, I.N.; Avsiyan, A.L.; Memetshaeva, N.O.A.; Lelekov, A.S.; Novikova, T.M. Production characteristics of *Dunaliella salina* in two-phase pilot cultivation (Crimea). *Turk. J. Fish. Aquat. Sci.* **2019**, *20*, 401–408. [[CrossRef](#)]
33. Wellburn, A.R. The spectral determination of chlorophylls a and b, as well as total carotenoids, using various solvents with spectrophotometers of different resolution. *J. Plant Physiol.* **1994**, *144*, 307–313. [[CrossRef](#)]
34. Jan, S.; Khan, M.R.; Rashid, U.; Bokhari, J. Assessment of antioxidant potential, total phenolics and flavonoids of different solvent fractions of *Monothecha buxifolia* fruit. *Osong Public Health Res. Perspect.* **2013**, *4*, 246–254. [[CrossRef](#)]
35. Safafar, H.; Van Wagenen, J.; Møller, P.; Jacobsen, C. Carotenoids, phenolic compounds and tocopherols contribute to the antioxidative properties of some microalgae species grown on industrial wastewater. *Mar. Drugs* **2015**, *13*, 7339–7356. [[CrossRef](#)] [[PubMed](#)]
36. Benzie, I.F.; Strain, J.J. Ferric reducing/antioxidant power assay: Direct measure of total antioxidant activity of biological fluids and modified version for simultaneous measurement of total antioxidant power and ascorbic acid concentration. In *Methods in Enzymology*; Packer, L., Ed.; Academic Press: Cambridge, MA, USA, 1999; Volume 299, pp. 15–27. [[CrossRef](#)]
37. Re, R.; Pellegrini, N.; Proteggente, A.; Pannala, A.; Yang, M.; Rice-Evans, C. Antioxidant activity applying an improved ABTS radical cation decolorization assay. *Free Radic. Biol. Med.* **1999**, *26*, 1231–1237. [[CrossRef](#)] [[PubMed](#)]
38. Guiry, M.D. *AlgaeBase*; World-Wide Electronic Publication, National University of Ireland: Galway, Ireland, 2013; Available online: <https://www.algaebase.org> (accessed on 9 March 2023).
39. Levasseur, W.; Perré, P.; Pozzobon, V. A review of high value-added molecules production by microalgae in light of the classification. *Biotechnol. Adv.* **2020**, *41*, 107545. [[CrossRef](#)]
40. Grubišić, M.; Šantek, B.; Zorić, Z.; Čošić, Z.; Vrana, I.; Gašparović, B.; Čož-Rakovac, R.; Ivančić Šantek, M. Bioprospecting of Microalgae Isolated from the Adriatic Sea: Characterization of Biomass, Pigment, Lipid and Fatty Acid Composition, and Antioxidant and Antimicrobial Activity. *Molecules* **2022**, *27*, 1248. [[CrossRef](#)]

41. Barten, R.J.; Wijffels, R.H.; Barbosa, M.J. Bioprospecting and characterization of temperature tolerant microalgae from Bonaire. *Algal Res.* **2020**, *50*, 102008. [[CrossRef](#)]
42. Ahmed, F.; Fanning, K.; Netzel, M.; Turner, W.; Li, Y.; Schenk, P.M. Profiling of carotenoids and antioxidant capacity of microalgae from subtropical coastal and brackish waters. *Food Chem.* **2014**, *165*, 300–306. [[CrossRef](#)]
43. Fon-Sing, S.; Borowitzka, M.A. Isolation and screening of euryhaline *Tetraselmis* spp. suitable for large-scale outdoor culture in hypersaline media for biofuels. *J. Appl. Phycol.* **2016**, *28*, 1–14. [[CrossRef](#)]
44. Lee, H.J.; Hur, S.B. Genetic relationships among multiple strains of the genus *Tetraselmis* based on partial 18S rDNA sequences. *Algae* **2009**, *24*, 205–212. [[CrossRef](#)]
45. González, M.A.; Aguayo, P.A.; Inostroza, I.D.L.; Castro, P.A.; Fuentes, G.A.; Gómez, P.I. Ultrastructural and molecular characterization of *Tetraselmis* strains (Chlorodendrophyceae, Chlorophyta) isolated from Chile. *Gayana Bot.* **2015**, *72*, 47–57. [[CrossRef](#)]
46. Hori, T.; Norris, R.E.; Chihara, M. Studies on the ultrastructure and taxonomy of the genus *Tetraselmis* (Prasinophyceae). I: Subgenus *Tetraselmis*. *Bot. Mag.* **1982**, *95*, 49–61. [[CrossRef](#)]
47. Hori, T.; Norris, R.E.; Chihara, M. Studies on the ultrastructure and taxonomy of the genus *Tetraselmis* (Prasinophyceae). III. Subgenus *Parvoiselmis*. *Bot. Mag.* **1986**, *99*, 123–135. [[CrossRef](#)]
48. Fučíková, K.; Leliaert, F.; Cooper, E.D.; Škaloud, P.; D’hondt, S.; De Clerck, O.; Gurgel, C.F.D.; Lewis, L.A.; Lewis, P.O.; Lopez-Bautista, J.M.; et al. New phylogenetic hypotheses for the core Chlorophyta based on chloroplast sequence data. *Front. Ecol. Evol.* **2014**, *2*, 63. [[CrossRef](#)]
49. Wang, Q.; Song, H.; Liu, X.; Liu, B.; Hu, Z.; Liu, G. Morphology and molecular phylogeny of coccoid green algae *Coelastrrella* sensu lato (Scenedesmeaceae, Sphaeropeales), including the description of three new species and two new varieties. *J. Phycol.* **2019**, *55*, 1290–1305. [[CrossRef](#)]
50. Nieves, M.; Voltolina, D.; Piña, P. Growth and biomass production of *Tetraselmis suecica* and *Dunaliella tertiolecta* in a standard medium added with three products of zeolitic nature. *Aquac. Eng.* **2005**, *32*, 403–410. [[CrossRef](#)]
51. Renaud, S.M.; Thinh, L.V.; Parry, D.L. The gross chemical composition and fatty acid composition of 18 species of tropical Australian microalgae for possible use in mariculture. *Aquaculture* **1999**, *170*, 147–159. [[CrossRef](#)]
52. Meseck, S.L.; Alix, J.H.; Wikfors, G.H. Photoperiod and light intensity effects on growth and utilization of nutrients by the aquaculture feed microalga, *Tetraselmis chuii* (LY429). *Aquaculture* **2005**, *246*, 393–404. [[CrossRef](#)]
53. Lim, D.K.Y.; Garg, S.; Timmins, M.; Zhang, E.S.; Thomas-Hall, S.R.; Schuhmann, H.; Li, Y.; Schenk, P.M. Isolation and evaluation of oil-producing microalgae from subtropical coastal and brackish waters. *PLoS ONE* **2012**, *7*, e40751. [[CrossRef](#)] [[PubMed](#)]
54. Fakhri, M.; Arifin, N.B.; Budianto, B.; Yuniarti, A.; Hariati, A.M. Effect of Salinity and Photoperiod on Growth of Microalgae *Nannochloropsis* sp. and *Tetraselmis* sp. *Nat. Environ. Pollut. Technol.* **2015**, *14*, 563.
55. Arkronrat, W.; Deemark, P.; Oniam, V. Growth performance and proximate composition of mixed cultures of marine microalgae (*Nannochloropsis* sp. & *Tetraselmis* sp.) with monocultures. *Songklanakarin J. Sci. Technol.* **2016**, *38*, 1–5.
56. Rafay, R.; Uratani, J.M.; Hernandez, H.H.; Rodríguez, J. Growth and Nitrate Uptake in *Nannochloropsis gaditana* and *Tetraselmis chuii* Cultures Grown in Sequential Batch Reactors. *Front. Mar. Sci.* **2020**, *7*, 77. [[CrossRef](#)]
57. Moussa, I.D.B.; Chtourou, H.; Karray, F.; Sayadi, S.; Dhouib, A. Nitrogen or phosphorus repletion strategies for enhancing lipid or carotenoid production from *Tetraselmis marina*. *Bioresour. Technol.* **2017**, *238*, 325–332. [[CrossRef](#)]
58. Kim, G.; Bae, J.; Lee, K. Nitrate repletion strategy for enhancing lipid production from marine microalga *Tetraselmis* sp. *Bioresour. Technol.* **2016**, *205*, 274–279. [[CrossRef](#)]
59. Adarme-Vega, T.C.; Thomas-Hall, S.R.; Lim, D.K.; Schenk, P.M. Effects of long chain fatty acid synthesis and associated gene expression in microalga *Tetraselmis* sp. *Mar. Drugs* **2014**, *12*, 3381–3398. [[CrossRef](#)]
60. Tsai, H.P.; Chuang, L.T.; Chen, C.N.N. Production of long chain omega-3 fatty acids and carotenoids in tropical areas by a new heat-tolerant microalga *Tetraselmis* sp. DS3. *Food Chem.* **2016**, *192*, 682–690. [[CrossRef](#)]
61. Fabregas, J.; Herrero, C.; Cabezas, B.; Abalde, J. Mass culture and biochemical variability of the marine microalga *Tetraselmis suecica* Kylin (Butch) with high nutrient concentrations. *Aquaculture* **1985**, *49*, 231–244. [[CrossRef](#)]
62. Sigaud, T.C.S.; Aidar, E. Salinity and temperature effects on the growth and chlorophyll- $\alpha$  content of some planktonic algae. *Bol. Inst. Oceanográfico* **1993**, *41*, 95–103. [[CrossRef](#)]
63. da Silva Gorgônio, C.M.; Aranda, D.A.G. Morphological and chemical aspects of *Chlorella pyrenoidosa*, *Dunaliella tertiolecta*, *Ischrysis galbana* and *Tetraselmis gracilis* microalgae. *Nat. Sci.* **2013**, *5*, 783–791. [[CrossRef](#)]
64. da Silva Ferreira, V.; Sant’Anna, C. Impact of culture conditions on the chlorophyll content of microalgae for biotechnological applications. *World J. Microbiol. Biotechnol.* **2017**, *33*, 20. [[CrossRef](#)] [[PubMed](#)]
65. Goiris, K.; Muylaert, K.; Fraeye, I.; Foubert, I.; De Brabanter, J.; De Cooman, L. Antioxidant potential of microalgae in relation to their phenolic and carotenoid content. *J. Appl. Phycol.* **2012**, *24*, 1477–1486. [[CrossRef](#)]
66. Stahl, W.; Sies, H. Antioxidant activity of carotenoids. *Mol. Aspects Med.* **2003**, *24*, 345–351. [[CrossRef](#)]
67. Young, A.J.; Lowe, G.L. Carotenoids—Antioxidant properties. *Antioxidants* **2018**, *7*, 28. [[CrossRef](#)]
68. Zhang, L.; Ravipati, A.S.; Koyyalamudi, S.R.; Jeong, S.C.; Reddy, N.; Smith, P.T.; Bartlett, J.; Shanmugam, K.; Münch, G.; Wu, M.J. Antioxidant and Anti-inflammatory Activities of Selected Medicinal Plants Containing Phenolic and Flavonoid Compounds. *J. Agric. Food Chem.* **2011**, *59*, 12361–12367. [[CrossRef](#)]
69. Huyut, Z.; Beydemir, Ş.; Gülçin, İ. Antioxidant and Antiradical Properties of Selected Flavonoids and Phenolic Compounds. *Biochem. Res. Int.* **2017**, *2017*, 7616791. [[CrossRef](#)]

70. Li, H.; Cheng, K.; Wong, C.; Fan, K.; Chen, F.; Jiang, Y. Evaluation of antioxidant capacity and total phenolic content of different fractions of selected microalgae. *Food Chem.* **2007**, *102*, 771–776. [[CrossRef](#)]
71. Hajimahmoodi, M.; Faramarzi, M.A.; Mohammadi, N.; Soltani, N.; Oveisi, M.R.; Nafissi-Varcheh, N. Evaluation of antioxidant properties and total phenolic contents of some strains of microalgae. *J. Appl. Phycol.* **2010**, *22*, 43–50. [[CrossRef](#)]
72. Bulut, O.; Akın, D.; Sönmez, Ç.; Öktem, A.; Yücel, M.; Öktem, H.A. Phenolic compounds, carotenoids, and antioxidant capacities of a thermo-tolerant *Scenedesmus* sp. (Chlorophyta) extracted with different solvents. *J. Appl. Phycol.* **2019**, *31*, 1675–1683. [[CrossRef](#)]
73. Mutha, R.E.; Tatiya, A.U.; Surana, S.J. Flavonoids as natural phenolic compounds and their role in therapeutics: An overview. *Futur. J. Pharm. Sci.* **2021**, *7*, 25. [[CrossRef](#)] [[PubMed](#)]
74. Assunção, M.F.G.; Amaral, R.; Martins, C.B.; Ferreira, J.D.; Ressurreição, S.; Santos, S.D.; Varejão, J.M.; Santos, L.M. Screening microalgae as potential sources of antioxidants. *J. Appl. Phycol.* **2017**, *29*, 865–877. [[CrossRef](#)]
75. Geetha, B.V.; Navasakthi, R.; Padmini, E. Investigation of antioxidant capacity and phytochemical composition of Sun *Chlorella*—An in vitro study. *J. Aquac. Res. Dev.* **2010**, *1*, 104. [[CrossRef](#)]
76. Custódio, L.; Justo, T.; Silvestre, L.; Barradas, A.; Duarte, C.V.; Pereira, H.; Barreira, L.; Rauter, A.P.; Alberício, F.; Varela, J. Microalgae of different phyla display antioxidant, metal chelating and acetylcholinesterase inhibitory activities. *Food Chem.* **2012**, *131*, 134–140. [[CrossRef](#)]
77. Goh, S.-H.; Yusoff, F.M.; Loh, S.-P. A comparison of the antioxidant properties and total phenolic content in a diatom, *Chaetoceros* sp. and a green microalga, *Nannochloropsis* sp. *J. Agr. Sci.* **2010**, *2*, 123–130. [[CrossRef](#)]
78. Monteiro, M.; Santos, R.A.; Iglesias, P.; Couto, A.; Serra, C.R.; Gouvinhas, I.; Barros, A.; Oliva-Teles, A.; Enes, P.; Díaz-Rosales, P. Effect of extraction method and solvent system on the phenolic content and antioxidant activity of selected macro-and microalgae extracts. *J. Appl. Phycol.* **2020**, *32*, 349–362. [[CrossRef](#)]

**Disclaimer/Publisher’s Note:** The statements, opinions and data contained in all publications are solely those of the individual author(s) and contributor(s) and not of MDPI and/or the editor(s). MDPI and/or the editor(s) disclaim responsibility for any injury to people or property resulting from any ideas, methods, instructions or products referred to in the content.